GEOPHYSICAL RESEARCH LETTERS, VOL. 28, NO. 23, PAGES 4383-4386, DECEMBER 1, 2001

Surface Wave Waveform Anomalies at the Saudi Seismic Network

G. Laske and N. Cotte

IGPP, Scripps Institution of Oceanography, University of California San Diego

Abstract. This paper describes surface wave waveforms observed at the Saudi Arabian Seismic Network. We identify records corresponding to events occuring in the Kuril Islands region as anomalous and discuss possible causes for the waveform distortions. Most likely, the waveform anomalies are caused by constructive and destructive interference of laterally refracted wave packets. Some waveform anomalies are probably of instrumental origin and we suspect a calibration error for the vertical component at station RIYD. For station AFIF, we find a significant clockwise rotation of the horizontal components with respect to geographic North by approximately 4 degrees.

Introduction

The recent increase of seismic data collected at permanent global seismic networks (e.g. GEOSCOPE, GSN) and regional permanent and temporary networks (e.g. MEDNET, passive seismic PASSCAL experiments) and the fact that these data are easily accessible through the IRIS data management center allows seismologists to construct global high-resolution images that have not been possible only a few years ago. An invaluable ingredient in crustal and upper mantle tomography using surface waves is the compilation of frequency-dependent dispersion maps (group or phase velocity) as an intermediate step (e.g. *Ekström et al.*, 1997). The construction of such maps is generally based on inverting measured group time delays or phase differences relative to synthetic waveforms. The large volume of available waveforms has inspired many workers to use automated algorithms rather than interactive screen routines to do the measurements (e.g. *Trampert and Woodhouse*, 1995). In most of such automated processes, the data analyst never sees individual waveforms. We show in a few examples that visually inspecting waveforms is an important step toward understanding how surface waves propagate in heterogeneous media and what other effects can cause observed waveform anomalies.

One reason why we analyze surface waves interactively is that apart from dispersion we also measure arrival angles [*Laske*, 1995]. In laterally heterogeneous media, surface waves get refracted away from the source-receiver great circle and arrive at the station at an angle that is different from the receiver-source azimuth. Rayleigh waves can then be seen on the transverse component and Love waves on the radial one. Measuring arrival angles involves inspection of the complete 3-component seismic records. High-quality arrival angle data therefore depend on a high signal-to-noise ratio on all three components and make the harvest of high-precision measurements more difficult than measuring dispersion. The great value of arrival angle measurements however originates in their enhanced sensitivity to short wavelength structure for a given source-receiver pair and a linear theory to relate such data to structure is readily available [*Woodhouse and Wong*, 1986]. We have sucessfully included arrival angles in inversions for global dispersion maps at long periods (longer than 60s; *Laske and Masters*, 1996) and have recently started to investigate the possibility to extend this process to shorter periods. In this paper, we identify cases for which making arrival angle measurements is not feasible. We inspect the corresponding waveforms and discuss what could cause the observed waveform anomalies.

Paper number 2001GL013364.
0094-8276/01/2001GL013364$05.00

The Dataset

The waveforms of this study were collected at the temporary Saudi Arabian Seismic Network (Figure 1; *Vernon et al.*, 1996). Our database includes waveforms for all shallow (source depth $<$ 150 km) events with seismic scalar moments, M_0, greater than $4 \cdot 10^{18}$ Nm (typically $M_s \geq 6.2$). We also include smaller events ($M_0 > 5{\cdot}10^{17}$ Nm) for epicentral distances closer than 95 degrees (typically $M_s \geq 5.2$). For the time of operation between November 1995 and February 1997 this gives 176 shallow, mainly teleseismic events. The raw 40 Hz data, which are available at the IRIS/DMC, are initially decimated to 1 Hz data and lowpass filtered with a corner period at 37s. The instrument responses as reported in the dataless SEED volumes are removed and the horizontal components are rotated into radial and transverse directions for each event. A quick inspection of the 3-component records reveals that arrival angle measurements for both Love and Rayleigh waves are possible for most events in the periods band (150 - 40s). A great majority of events are at epicentral distances 60–95 degrees from the Saudi Network. Significant multipathing can occur over such long distances and collecting data at periods significantly shorter than 40s often seems not feasible. Where possible we measure the frequency–dependent arrival angles using a multi-taper technique. The essential step is a singular value decomposition using the spectra of all three components (see *Laske*, 1995 for details). The final dataset includes 384 high–quality measurements that will constrain near–receiver, short–wavelength structure in a future tomographic study. Here we concentrate on cases for which taking measurements is not possible. Measuring arrival angles is straightforward if Rayleigh and Love waves are clearly separated in time, i.e. the source–receiver path–averaged group velocities have to be sufficiently different. We notice that this is not the case for events occuring along the western Pacific subduction trenches between the Western Aleutian Islands and Taiwan. An example is shown in

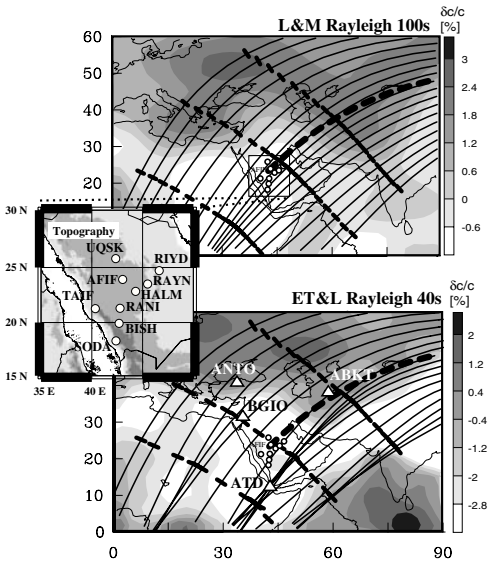

Figure 1. Map of the temporary Saudi Arabian Seismic Network [Vernon et al., 1996]. Also shown are sections of the global Rayleigh wave phase velocity maps of *Laske and Masters* [1996] at 100s and of *Ekström et al.* [1997] at 40s. Thick dashed lines mark the source-receiver great circle for the event of Figure 2 and station AFIF. Thin lines are rays traced through both maps and intermediate dashed lines mark snapshots of the propagating wavefronts. White triangles mark GSN stations that are closest to the Saudi Network.

Figure 2. These events have receiver–source azimuths between 30 and 90 degrees and the travel paths are almost purely continental. The group velocities calculated for isoptropic PREM [*Dziewonski and Anderson*, 1981] in which the crust is replaced by a 39km thick continental crust are 3.74 and 3.63km/s for Love and Rayleigh waves at 40s which is too similar to separate the wave trains sufficiently. On the other hand, the velocities at 55s are 3.97 and 3.80km/s which gives the required separation. That this is indeed the case is confirmed by lowpass filtering the data (corner period at 50s) for which the Love waves clearly compose the leading wave train.

Recordings from the Kuril Islands

We routinely calculate synthetic mode summation seismograms, since they are needed when measuring phase anomalies [*Laske and Masters*, 1996]. Though such seismograms are quite simple, they are useful tools to identify unusual waveforms. We use modfied PREM (see above), the PDE source locations and the Harvard CMT solutions as source mechanisms. Sometimes the signal on the transverse component is surprisingly large and significantly delayed with respect to the synthetic arrivals (e.g. BISH in Figure 2). Simple effects due to structural variations (i.e. decreased attenuation in an anomalously slow region) seem unlikely because the waveforms at adjacent stations (i.e. AFIF) do not display the same amplified signals despite the great similarity in travel paths. Records from events in the Kuril Islands region (about 20 events) are intriguing since the Love waves are predicted to be significantly smaller at the Saudi Network than the Rayleigh waves (Figures 2 and 3). We notice that at station BISH the high-frequency content of the vertical and radial components is reduced, while it is increased on the transverse component. It is relatively difficult to transfer Rayleigh wave energy from the vertical to the transverse component. An effective mechanism is Rayleigh–Love wave coupling caused by strong lateral gradients in azimuthal anisotropy (e.g. *Park and Yu*, 1992). The proof of this for our case is beyond the scope of this paper. We rather focus our attention on a more straightforward candidate for waveform distortions on the horizontal components: ray bending and interference of wave packets that are laterally refracted in a heterogeneous isotropic medium. Variations in phase travel time along different rays that pass a station could lead to destructive or constructive interference. The anomalous wave packets on the transverse component can either be strongly scattered Love waves (which arrive later than the direct Love wave) or refracted Rayleigh waves which arrive at about the same time as the direct Rayleigh wave.

We estimate the effects caused by lateral refraction by performing 2D ray tracing at long and short periods using the phase velocity maps of *Laske and Masters* [1996] at 100s and of *Ekström et al.* [1997] at 40s (Figure 1). The resulting ray geometries clearly indicate that while at long periods incoming wavefronts are barely distorted, significant lateral refraction occurs at short periods. A long segment of the ray path between the Kuril Islands and the Saudi Network passes the large low-velocity anomaly associated with the Tibetan Plateau and China at gracing angles which leads

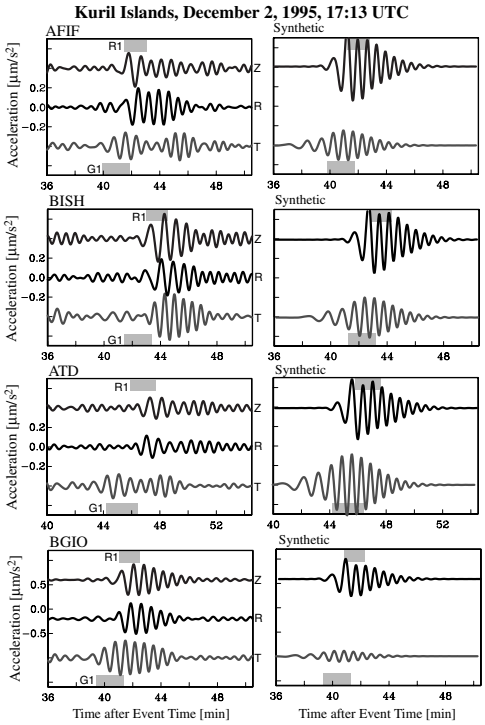

Figure 2. Left: Three-component records of the Dec 2, 1995 Kuril Islands event at Saudi stations AFIF and BISH, at GEOSCOPE station ATD (Arta Cave, Djibouti) and GEOFON station BGIO (Bar Giyyora, Israel). Right: mode summation synthetic seismograms for the vertical and transverse components using modified PREM. Grey bars mark theoretical arrivals for periods between 50 and 40s for Rayleigh (R1) and Love (G1) waves. The scale at BGIO is roughly twice that for the other stations.

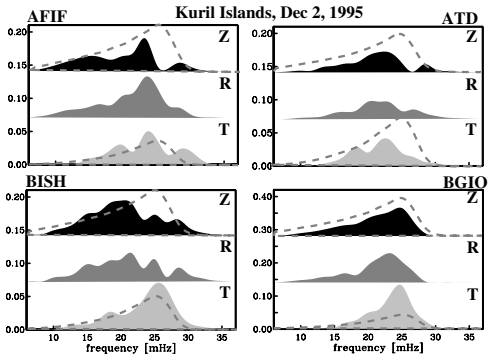

Figure 3. Spectra of the observed wave trains of Figure 2. Dashed lines mark spectra of the synthetic waveforms. The amplitude axis at BGIO is twice that of the other stations. All spectra were calculated using a boxcar window and the same window length.

to several caustics further down the path. The most prominent focusing of rays occurs just to the south of the Saudi Network. Significant differences in waveform distortions between AFIF and BISH may require a slight northward shift of the whole set of rays, implying a slight shift of the anomalies that causes the ray bending. The caustic found for 40s Rayleigh waves moves north from ATD toward BISH as the period increases to 60s (using the Harvard phase velocity maps). The caustic for 40s Love waves is similar to that for Rayleigh waves but it disperses with increasing period and a part moves into the Persian Gulf. One might expect that focusing of rays near GEOSCOPE station ATD leads to strong interference. Indeed, the waveforms at ATD appear particularly distorted and we suspect severe destructive interference as the cause (Figures 2 and 3). The reduced amplitudes are somewhat puzzling as the ray tracing actually predicts constructive interference at 40s. The amplitudes at ATD are quite often reduced relative to synthetic seismograms initially suggesting a calibration error. Careful analysis of all Nov95-Feb97 events reveal however that the observed effects depend on the source geography and are therefore not likely of instrumental cause. The same is true for unusually large Love waves at station BGIO. The waveforms at BGIO do not appear to be distorted which is consistent with the ray tracing predictions in Figure 1. We notice that BGIO is often close to a node in the source radiation pattern and Love wave amplitudes at BGIO may change quickly with slight changes in the moment tensor.

A useful tool to identify events for which serious multipathing is to be expected is the difference between arrival angles obtained from two-point ray tracing on one hand and using the linear path integral approximation, PIA, of *Woodhouse and Wong* [1986] on the other. We assume a difference of 3 degrees or greater as unacceptable. In a systematic ray tracing experiment we define fictitious sources on a fine polar grid with station AFIF being at the center and determine the arrival angles using ray tracing and the PIA (Figure 4). At a period of 100s, multipathing becomes significant only for sources with epicentral distances beyond 165° (except for events in Central America). At 40s however, multipathing can be severe for sources along the Western Pacific subduction trenches and beyond. This supports our observation that Kuril Islands events recorded at the Saudi Network exhibit anomalous waveforms.

Source Effects

An interesting pair of events are two Kuril Islands events on December 10, 1995 (22:22 and 22:48 UTC). The waveforms at the Saudi Network of these events are practically overlays of each other, except for a time shift of about 7s, when assuming the source locations and event times listed in the PDE catalog (the sources are about 14km apart). A shift is also seen for body wave phases though it is somewhat less. A discrepancy of 7s implies dispersion anomalies (path-averaged phase but also group velocity) of up to 0.5%. These shifts disappear completely when adopting the REB information instead of the PDE information. REB information ("Reviewed Event Bulletin") is issued by the Center for Monitoring Research and was temporarily used at the end of 1995 in the Harvard CMT catalog (Ekström, personal communication). An inspection of the complete set of GSN waveforms for these events reveals that the majority of waveforms that match when using the PDE locations are those of stations in the U.S.. We therefore conclude that the REB locations are more consistent with global long-period waveforms observed for these events. The major difference between the REB and the PDE information is that the second event in the REB was located 20 km further west, relative to the first location, and occured about 2 s later relative to the first event. These discrepancies in event information seem hardly significant and can, in general, not be verified due to the lack of similar event clusters. This example demonstrates however, that relatively small uncertainties in source information can imply relatively large uncertanties in surface wave dispersion for individual source–receiver pairs.

Instrumental Effects

Quite similar to ATD, we find reduced amplitudes at Saudi station RIYD. For RIYD, however, *all* Rayleigh wave amplitudes on the vertical component are reduced by a factor of roughly 2, regardless of epicentral distance or source azimuth. At the same time, the Love wave amplitudes on the transverse component appear normal. We therefore suspect that the calibration factor of the vertical component at RIYD is too large by a factor of roughly 2.

Surface wave arrival angles are sensitive to laterally heterogeneous seismic structure as well as instrument calibration errors and misalignment with Geographic North. It is straightforward to include an apparent misorientation at

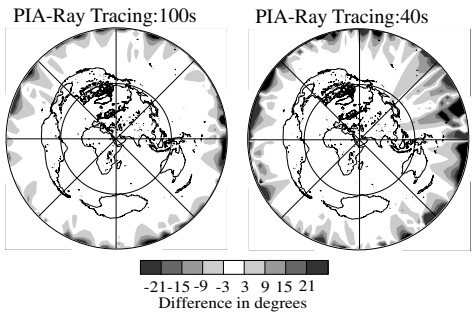

Figure 4. Difference between arrival angles predicted using the path integral approximation (PIA) and 2-point ray tracing, at two periods. The values are plotted as function of epicentral distance and receiver–source azimuth in a polar diagram. The inner circle marks epicentral distances of 90 degrees.

Table 1. Component Misalignment Expressed as Apparent North

Station	# Data Rayleigh	# Data Love	Apparent North [deg]	Comment
AFIF	43	37	-4.22 ± 0.66	
BISH	4	4	0.52 ± 1.35	1)
HALM	16	16	-1.65 ± 0.84	
RANI	18	21	-2.76 ± 0.96	
RAYN	19	21	1.71 ± 0.87	
RIYD	4	5	0.70 ± 1.34	2)
SODA	70	78	-2.72 ± 0.54	
TAIF	7	10	-4.01 ± 1.66	2)
UQSK	3	8	-4.04 ± 2.52	2)

Apparent North is the angle at which true North appears with respect to the N component of an instrument. Negative values imply a clockwise rotation of the equipment.
1) uncertain; stolen after 2 weeks
2) uncertain; late installation

each site as additional model parameter in a joint inversion for structure [*Laske*, 1995], assuming orthogonality of the horizontal components. The component orientation does not depend on wave type or frequency, so inversions for Love and Rayleigh waves performed at different periods should yield the same results. To increase accuracy we perform joint inversions for 3 periods between 150 and 80s for both wave types and then average the results. Only long periods are used because the increasing contribution from short-wavelength structure could potentially introduce a bias at shorter periods, especially for stations with uneven data coverage. Table 1 summarizes the component misalignment for the stations of the Saudi Network. We obtain stable results for at least 4 of the 9 stations (AFIF, RANI, RAYN and SODA). The components at station AFIF are significantly rotated with respect to true North, by approximately 4°. This value appears small and the reader may be tempted to conclude that this is insignificant. Note however that surface wave arrival angles predicted using current global phase velocity maps are typically not larger than this. It is also worth mentioning that shear wave splitting parameters also depend on component misalignment. Splitting data at station AFIF are found to be anomalous [*Wolfe et al.*, 1999] an some of the station misalignment could have mapped into this result. The number of data at stations BISH, RIYD and TAIF is low which is reflected in the larger error bar for the misalignment. However, at TAIF it appears to be at least 2.5°. The value for station UQSK is uncertain as the few available measurements have large error bars and Love and Rayleigh wave angles appear to be inconsistent.

Discussion

We have observed surface wave waveform anomalies at the Saudi Arabian Seismic Network and discussed possible causes for events occuring in the Kuril Islands region. Ray tracing experiments show that current global phase velocity maps indeed predict distortions of the incoming wavefield near the Saudi Network, the most likely cause for the distortion being the large-scale low-velocity anomaly surrounding the Tibetan Plateau and China. In further experiments, we have constructed phase velocity maps using our current crustal model (CRUST 2.0; http://mahi.ucsd.edu/Gabi) and the Scripps mantle model SB4L18 [*Masters et al.*, 2000]. Crustal structure alone cannot produce anomalies that bend rays as much as observed with current phase velocity maps. A combination of three times the uppermost 100km of SB4L18 (a model that is *not* designed to fit short periods surface waves) and CRUST 2.0, however, reproduces what we see for the Ekström et al. map at 40s.

We find two cases for which waveform anomalies are caused by instrumental problems: 1) the calibration constant of the Z–component at RIYD is too large by a factor of rougly two; 2) the horizontal components at AFIF are rotated clockwise with respect to true North by more than 4° .

Acknowledgments. We thank the network operator of the Saudi Seismic Network, Dr. Frank Vernon, for providing the dataset and the IRIS-DMC for easy standardized access to the data. Thanks to Göran Ekström and Jeff Park for helpful discussions and to an anonymous reviewer. This research was financed by National Science Foundation grants EAR-97-06056 and SAIC subcontract 44000025260.

References

Dziewonski, A.M., and D.L. Anderson Preliminary reference Earth model *Phys. Earth Planet. Inter., 25,* 297–356, 1981.
Ekström, G., J. Tromp, and E.W. Larson, Measurements and models of global models of surface wave propagation, *J. Geophys. Res., 102,* 8137–8157, 1997.
Laske, G., Global observation of off-great circle propagation of long-period surface waves, Geophy. J. Int., *123,* 245–259, 1995.
Laske, G., and G. Masters, Constraints on global phase velocity maps by long-period polarization data, *J. Geophys. Res., 101,* 16,059–16,075, 1996.
Masters, G., Laske, G., Bolton, H., and A. Dziewonski, The Relative Behavior of Shear Velocity, Bulk Sound Speed, and Compressional Velocity in the Mantle: Implications for Chemical and Thermal Structure, in *Earth's Deep Interior: Mineral Physics and Tomography From the Atomic to the Global Scale,* AGU Monograph 117, edited by S. Karato, A.M. Forte, R.C. Liebermann, G. Masters and L. Stixrude, pp. 63–87, AGU, Washington, D.C., 2000.
Park, J., and Y. Yu, Anisotropy and coupled free oscillations: simplified models and surface wave observations, Geophy. J. Int., *110,* 401–420, 1992.
Trampert, J., and J.H. Woodhouse, High-resolution global phase velocity distribution, *Geophys. Res. Lett., 23,* 21–24, 1996.
Vernon, F., R.J. Mellors, J. Berger, A.M. Al-Amri, and J. Zollweg, Initial results from the deployment of broad-band seismometers in the Saudi Arabian Shield, *Proc. of the 18th Annual DOE Seismic Research Symposium*, Sep 4-6, Annapolis, Maryland, 108–117, 1996.
Wolfe, C.J., Vernon III, F.L., and A. Al–Amri Shear–wave splitting across western Saudi Arabia: The pattern of upper mantle anisotropy at a Proterozoic shield *Geophys. Res. Lett., 26,* 779–782, 1999.
Woodhouse, J.H., and Y.K. Wong, Amplitude, phase and path anomalies of mantle waves, *Geophys. J. R. Astron. Soc., 87,* 753–773, 1986.

G. Laske and N. Cotte, IGPP, Scripps Institution of Oceanography, University of California San Diego, CA 92093-0225 (e-mail: glaske@ucsd.edu)

(Received April 27, 2001; revised July 12, 2001;
accepted September 05, 2001.)